

Supporting Information

I. Experimental Section

Catalyst synthesis. $\text{SrCo}_{0.5}\text{Fe}_{0.5}\text{O}_{3-\delta}$ (SCF) perovskite oxide was synthesized by a combined ethylenediaminetetraacetic acid-citric acid (EDTA-CA) complexing sol-gel method. Stoichiometric amounts of $\text{Sr}(\text{NO}_3)_2$, $\text{Co}(\text{NO}_3)_2 \cdot 6\text{H}_2\text{O}$ and $\text{Fe}(\text{NO}_3)_3 \cdot 9\text{H}_2\text{O}$ were mixed in deionized water. EDTA and citric acid were then added as complexing agents in sequence at a mole ratio of 1:1:2 for total metal ions/EDTA/citric acid. To ensure complete complexation, the pH of the solution was adjusted to 6-7 by the addition of NH_3 aqueous solution. A transparent gel was obtained by heating at 90 °C under stirring. The gel was then heated in the furnace at 250 °C for 5 h in air to form a solid precursor. Finally, the solid precursor was calcined at 600, 800, 1000 and 1200 °C for 5 h in air to form SCF-600, SCF-800, SCF-1000 and SCF-1200 powders, respectively. The other metal oxides used in this study, namely, LaCoO_3 (LC), $\text{Ca}_2\text{CoFeO}_5$ (CCF) and $\text{Ba}_{0.5}\text{Sr}_{0.5}\text{Co}_{0.8}\text{Fe}_{0.2}\text{O}_{3-\delta}$ (BSCF) were also synthesized by the identical procedure as SCF, with the exception of the distinction of their amounts of raw materials. The RuO_2 catalyst in this work was purchased from Sigma-Aldrich.

Characterization. XRD patterns were collected using an X-ray diffractometer (D8 Advance, Bruker, Germany) equipped with filtered $\text{Cu-K}\alpha$ radiation ($\lambda = 1.5418 \text{ \AA}$) by step scanning with an interval of 0.02° in the 2θ range of $20\text{-}80^\circ$. SAED pattern and the corresponding HRTEM image were obtained using FEI Tecnai G2 F20 operated at an accelerating voltage of 200 kV. SEM images were obtained on a field-emission scanning electron microscope (FEI Nova Nano-SEM 450). Nitrogen sorption isotherms were measured at 77 K with a Micromeritic Tri Flex surface characterization analyzer and the specific surface areas were calculated by using the BET method. XPS experiments were carried out on the Nexsa surface analysis system with $\text{Al K}\alpha$ X-ray source for radiation and data were fitted by the public software package XPSPEAK. Soft XAS was performed at the 11A beam line of the NSRRC in Taiwan. The $\text{Co-L}_{2,3}$, $\text{Fe-L}_{2,3}$ and O-K XAS spectra were obtained using the TEY mode. To calibrate the energy scale, NiO , CoO and Fe_2O_3 single crystals were measured simultaneously for the O-K , $\text{Co-L}_{2,3}$ and $\text{Fe-L}_{2,3}$ edges, respectively.

Electrode Preparation. Working electrodes for OER tests were prepared by a controlled drop-casting method on a RDE (Pine Research Instrumentation, 5 mm diameter). The RDE was pre-polished with aqueous alumina suspension on a polishing cloth. To eliminate the electrode conductivity restriction within thin film working electrodes, the catalysts in this work were mixed with as-obtained

conductive carbon (Super P Li) at a mass ratio of 1:1. Briefly, a 6 μL aliquot of the catalyst ink, which was prepared by sonication of a mixture of 10 mg of oxide powder and 10 mg of conductive carbon dispersed in 1 mL ethanol and 100 μL of 5 wt% Nafion solution for at least 1 h, was dropped on the electrode surface, generating an approximate catalyst loading of $0.556 \text{ mg}_{\text{total}} \text{ cm}^{-2}$ ($0.278 \text{ mg}_{\text{oxide}} \text{ cm}^{-2}$) and was left to dry before the electrochemical tests.

Electrochemical measurements. OER activity in 0.1 M KOH solution was conducted using in a standard three-electrode electrochemical cell (Pine Research Instrumentation) with an RDE configuration controlled by a CHI 760E electrochemistry workstation. Catalysts cast on RDE, Pt foil and Ag|AgCl (3.5M KCl) were used as the working electrode, counter electrode, and reference electrode, respectively. During the measurement, RDE electrode was constantly rotating at 1600 rpm to get rid of the bubbles. The electrolyte was bubbled with O_2 for ~ 30 min prior to OER measurements and maintained under O_2 atmosphere throughout the test period. OER polarization curves were collected by capacitance-corrected cyclic voltammetry (CV) curves at a scan rate of 10 mV s^{-1} from 0.2 to 0.8 V vs. Ag|AgCl. Polarization curves were iR corrected in this work unless noted otherwise. The polarization curves were replotted as overpotential (η) versus the logarithm of current density ($\log |J|$) to obtain Tafel plots. The chronopotentiometry tests were conducted at a constant current density of 10 mA cm^{-2} . CV method was used to measure the electrochemical double layer capacitance. The potential was swept at different scan rates of 20, 40, 60, 80 and 100 mV s^{-1} from 0.2 to 0.3 V vs. Ag|AgCl, where no faradic current was observed. The halves of the positive and negative current density differences at the center of the scanning potential range (i.e., 0.25 V) were plotted versus scan rates where the slopes represent the double layer capacitance.

II. Supplementary Results

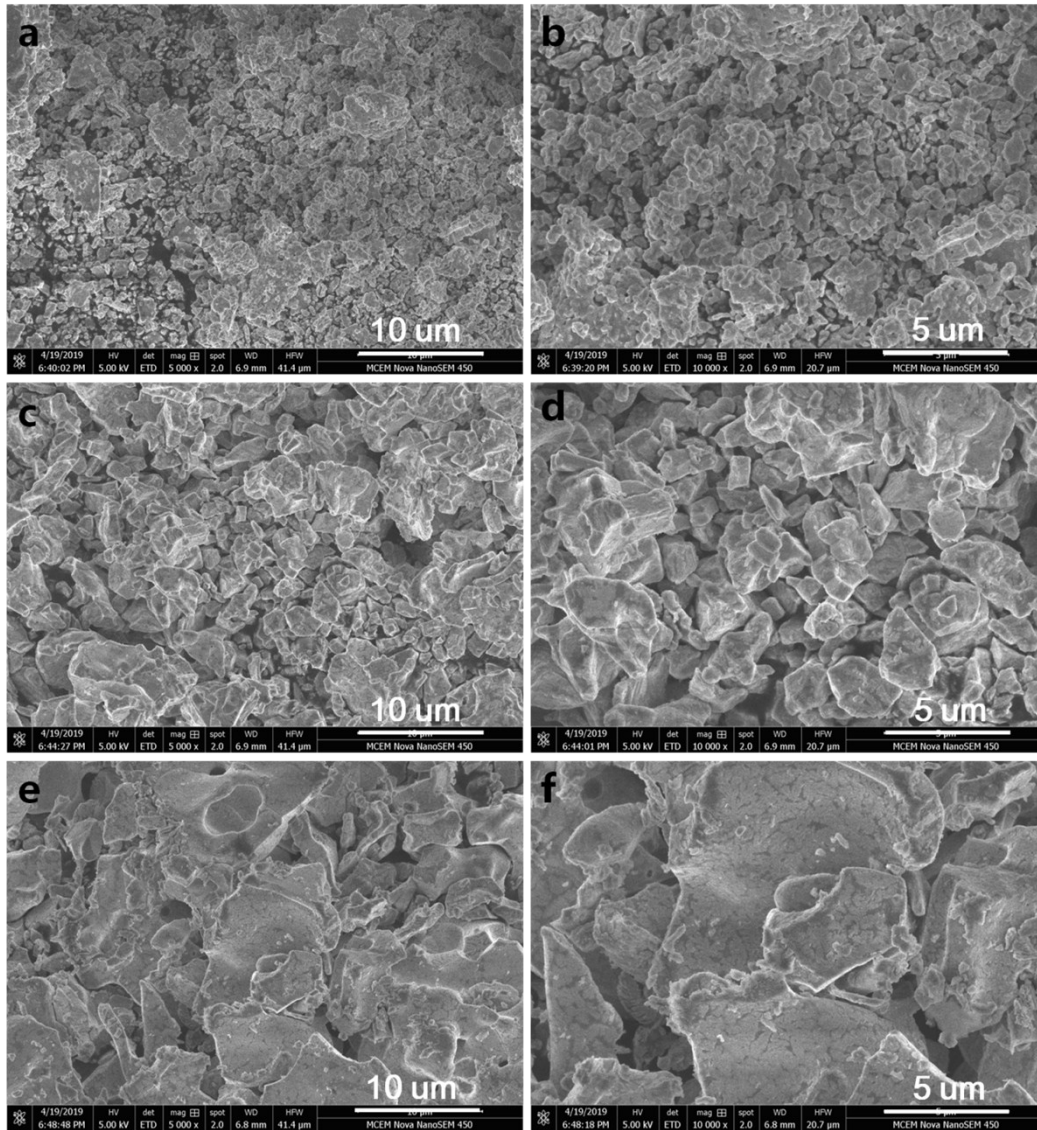


Fig. S1. SEM images of (a,b) SCF-800, (c,d) SCF-1000 and (e,f) SCF-1200 with different magnifications.

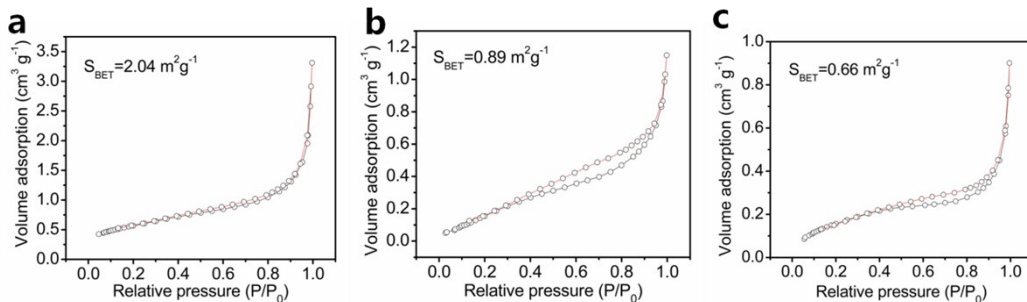


Fig. S2. N₂ adsorption-desorption isotherm of (a) SCF-800, (b) SCF-1000 and (c) SCF-1200.

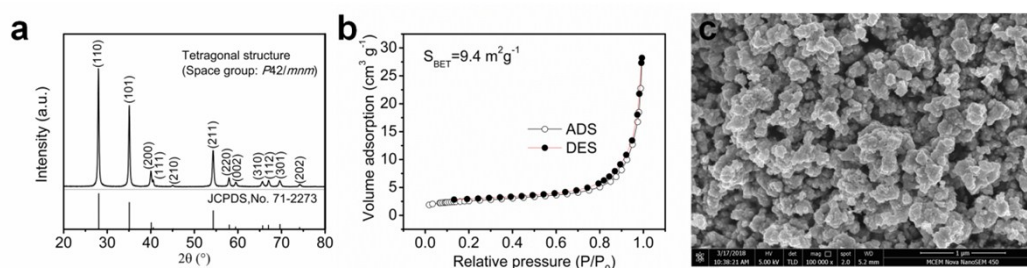


Fig. S3. (a) XRD patterns of commercial RuO₂ powder (Sigma-Aldrich). (b) N₂ adsorption-desorption isotherm of RuO₂. (c) SEM image of RuO₂.^[S1]

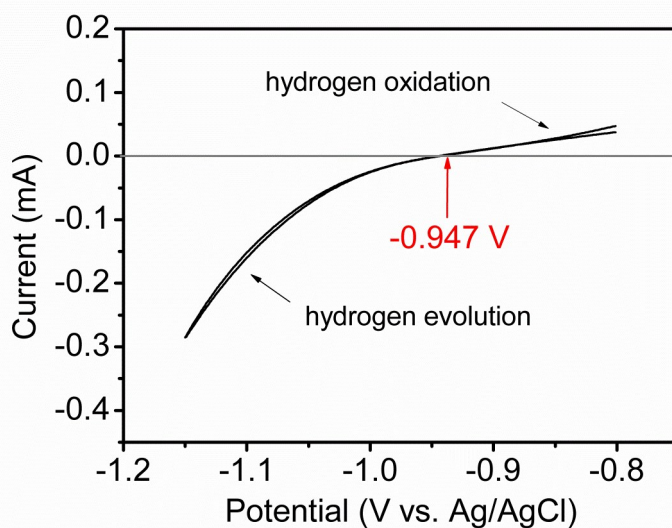


Fig. S4. Potential calibration of the Ag/AgCl reference electrode in 0.1 M KOH solution. The calibration was performed in a high purity hydrogen-saturated electrolyte with a platinum rotating disk electrode (PINE, 4 mm diameter, 0.126 cm²) as the working electrode. Cyclic voltammetry (CV) was run at a scan rate of 1 mV s⁻¹, and the average of the two potentials at which the current crossed zero was taken to be the thermodynamic potential for the hydrogen electrode reaction. In 0.1 M KOH, $E_{\text{RHE}} = E_{\text{Ag/AgCl}} + 0.947 \text{ V}$.^[S2]

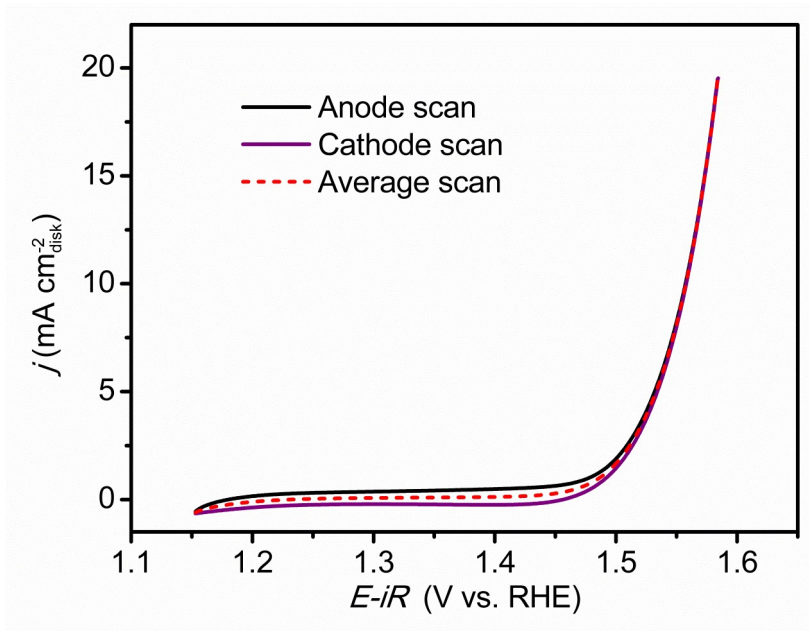


Fig. S5. Capacitive correction of the as-measured CV curve (10 mV s^{-1}) of example catalyst (i.e., SCF-800).

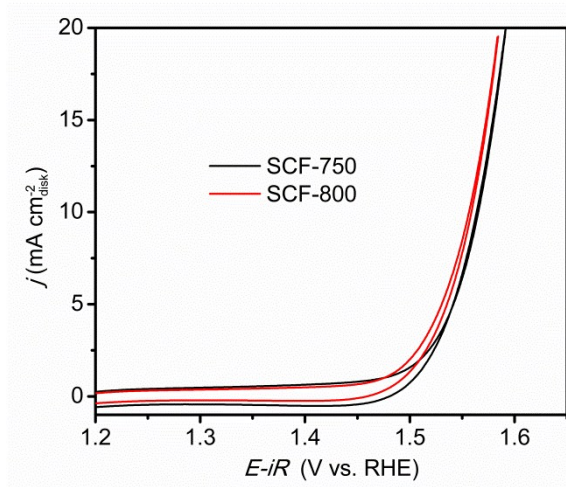


Fig. S6. CV curves of SCF-750 and SCF-800 catalysts in O_2 -saturated 0.1 M KOH solution.

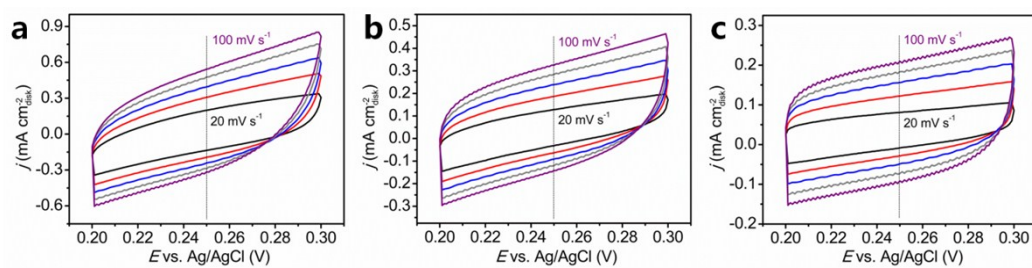


Fig. S7. CV measurements in a non-faradic current region (0.2-0.3 V vs. Ag/AgCl) at scan rates of 20, 40, 60, 80 and 100 mV s^{-1} of (a) SCF-800, (b) SCF-1000 and (c) SCF-1200 catalysts in 0.1 M KOH solution.

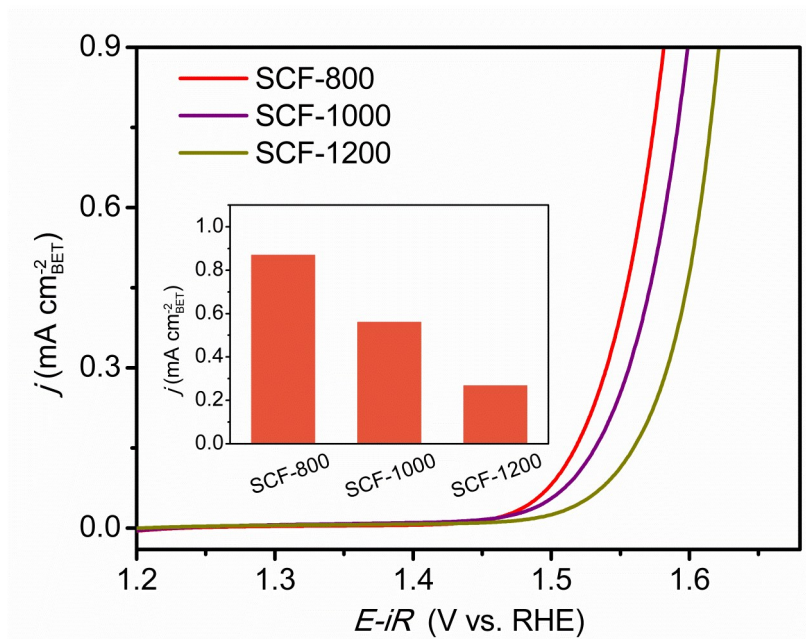


Fig. S8. Specific activity normalized to BET surface area of SCF-T catalysts as a function of potential. Inset: specific activity at the overpotential of $\eta=0.35$ V.

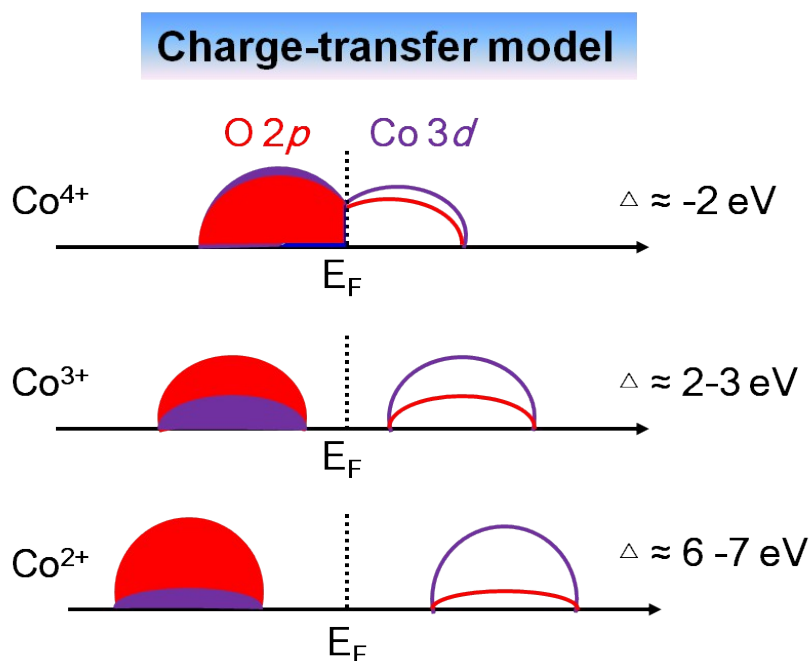


Fig. S9. Charge-transfer models of Co^{2+} , Co^{3+} and Co^{4+} in covalent systems [S3-S5].

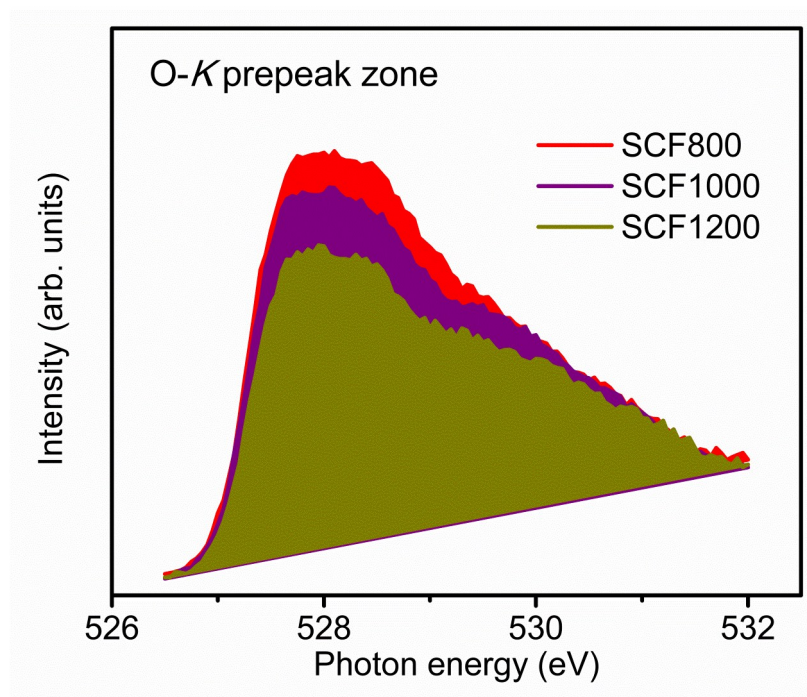


Fig. S10. O-K XAS prepeak region (from 526.5 to 532 eV) for SCF-T.

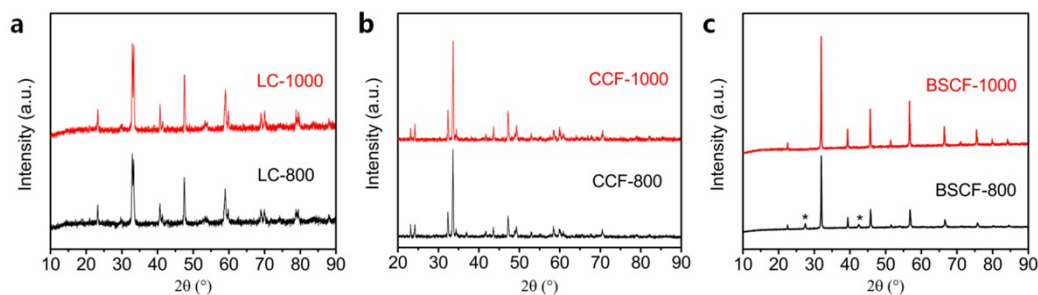


Fig. S11. XRD patterns of (a) LC, (b) CCF and (c) BSCF samples. * indicates a tiny impurity peak in BSCF-800.

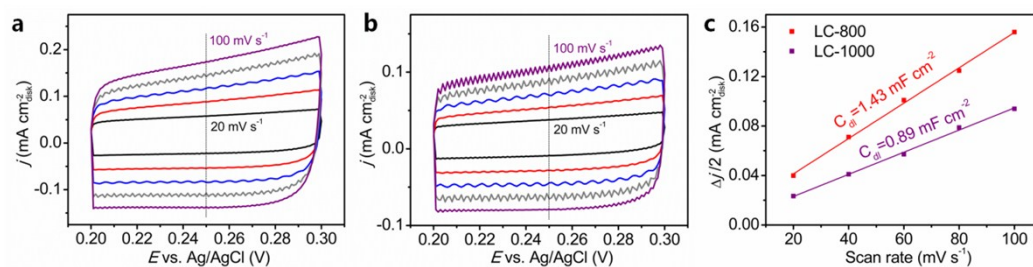


Fig. S12. CV measurements in a non-faradic current region (0.2-0.3 V vs. Ag/AgCl) at scan rates of 20, 40, 60, 80 and 100 mV s^{-1} of (a) LC-800 and (b) LC-1000 catalysts in 0.1 M KOH solution. (c) Linear fitting curves of the capacitive currents versus CV scan rates for LC-800 and LC-1000 catalysts.

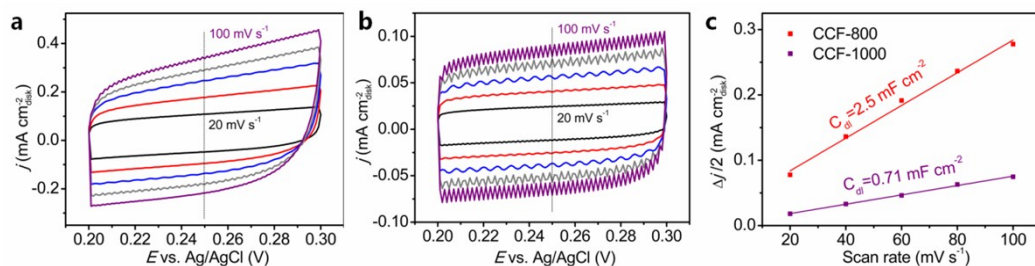


Fig. S13. CV measurements in a non-faradic current region (0.2-0.3 V vs. Ag/AgCl) at scan rates of 20, 40, 60, 80 and 100 mV s^{-1} of (a) CCF-800 and (b) CCF-1000 catalysts in 0.1 M KOH solution. (c) Linear fitting curves of the capacitive currents versus CV scan rates for CCF-800 and CCF-1000 catalysts.

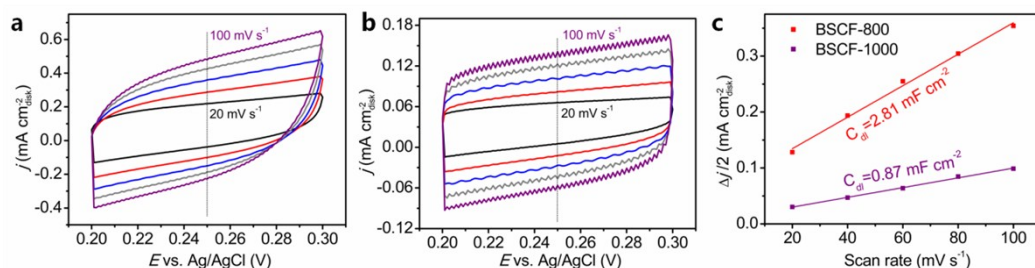


Fig. S14. CV measurements in a non-faradic current region (0.2-0.3 V vs. Ag/AgCl) at scan rates of 20, 40, 60, 80 and 100 mV s^{-1} of (a) BSCF-800 and (b) BSCF-1000 catalysts in 0.1 M KOH solution. (c) Linear fitting curves of the capacitive currents versus CV scan rates for BSCF-800 and BSCF-1000 catalysts.

Table S1. Comprehensive comparison of OER activity among SCF-T catalysts.

Catalysts	η @ 10 mA cm^{-2} (mV)	Tafel slope (mV dec^{-1})	C_{dl} (mF cm^{-2})	Mass activity @ $\eta=0.35$ V ($\text{A g}^{-1}_{\text{oxide}}$)	Specific activity @ $\eta=0.35$ V ($\text{mA cm}^{-2}_{\text{ECSA}}$)	Specific activity @ $\eta=0.35$ V ($\text{mA cm}^{-2}_{\text{BET}}$)
SCF-800	327	62	3.29	63.5	0.2	0.87
SCF-1000	377	74	1.92	18.0	0.1	0.56
SCF-1200	409	76	1.32	6.4	0.05	0.27

Table S2. Comparison of OER activity for SCF-800 with reported state-of-the-art perovskite-based catalysts supported on glass carbon electrode in 0.1 M KOH.

Catalysts	Mass loading (mg cm ⁻²)	η @ 10 mA cm ⁻² (mV)	Mass activity @ $\eta=0.35$ V (A g ⁻¹)	References
SCFN-800	0.278	327	63.5	This work
Nd _{1.5} Ba _{1.5} CoFeMnO _{9-δ} (NBCFM)	0.209	359	~21	<i>Sci. Adv.</i> 2018, 4, eaap9360
SrCoO _{2.7}	0.0153	419	~144	<i>Nat. Commun.</i> , 2018, 9, 3150
La _{0.5} Sr _{1.5} Ni _{0.7} Fe _{0.3} O _{4.04} (RP- LSNF)	0.0153	360	~177	<i>Nat. Commun.</i> , 2018, 9, 3150
p-SnNiFe	0.25	350	~40	<i>Nat. Commun.</i> 2017, 8, 394
PrBa _{0.5} Sr _{0.5} Co _{1.5} Fe _{0.5} O _{5+δ} Nanofiber (PBSCF NF)	0.202	358	~40	<i>Nat. Commun.</i> 2017, 8, 14586
80nm LaCoO ₃	0.25	490	~0.9	<i>Nat. Commun.</i> 2016, 7, 11510
CaCu ₃ Fe ₄ O ₁₂	0.25	~370	~6.8	<i>Nat. Commun.</i> 2015, 6, 8249
Pr _{0.5} Ba _{0.5} CoO _{3-δ} (PBC)	0.25	~400	~7	<i>Nat. Commun.</i> 2013, 4, 2439
La _{0.5} Ba _{0.25} Sr _{0.25} CoO _{2.9-δ} F _{0.1} (LBSCF0.1)	0.157	~470	~11	<i>Chem</i> 2018, 4, 2902
Bi ₇ Co ₃ Ti ₃ O ₂₁	0.38	~470	~2	<i>J. Am. Chem. Soc.</i> 2019, 141, 3121
BaN _{10.83} O _{2.50}	0.295	~420	~6	<i>J. Am. Chem. Soc.</i> 2016, 138, 3541
Co ₃ O ₄ /La _{0.3} Sr _{0.7} CoO ₃ (LSC)	0.25	~380	~19	<i>Angew. Chem. Int. Ed.</i> 2019, 131, 11846
SrNb _{0.1} Co _{0.7} Fe _{0.2} O _{3-δ} (SNCF)	0.232	500	~4	<i>Angew. Chem. Int. Ed.</i> 2015, 54, 3897
Ca _{0.9} Yb _{0.1} MnO _{2.65} (CYM)	N.A.	~470	N.A.	<i>Adv. Mater.</i> 2015, 27, 5989
O ₂ treated Ba _{0.5} Sr _{0.5} Co _{0.8} Fe _{0.2} O _{3-δ} (O ₂ -BSCF)	0.639	550	~1.2	<i>Adv. Mater.</i> 2015, 27, 266
La _{0.7} (Ba _{0.5} Sr _{0.5}) _{0.3} Co _{0.8} Fe _{0.2} O _{3-δ} -50 nm (LBSCF-50 nm)	0.639	~370	~44	<i>Energy Environ. Sci.</i> 2016, 9, 176
Sr(Co _{0.8} Fe _{0.2}) _{0.7} B _{0.3} O _{3-δ} (SCFB-0.3)	0.232	340	~58	<i>Adv. Energy Mater.</i> 2019, 9, 1900429

CaMnO ₃ /S-300	0.1	470	~16	<i>Adv. Energy Mater.</i> 2018, 8, 1800612
SrNb _{0.1} Co _{0.7} Fe _{0.2} O _{3-δ} nanorod (SNCF NR)	0.232	389	~14	<i>Adv. Energy Mater.</i> 2017, 7, 1602122
SrCo _{0.95} P _{0.05} O _{3-δ} (SCP)	0.232	480	~1.2	<i>Adv. Funct. Mater.</i> 2016, 26, 5862
LaFe _{1-x} P _x O _{3-δ} -500	0.255	465	N.A.	<i>Nano Energy</i> 2018, 47, 199
LaSr ₃ Co _{1.5} Fe _{1.5} O _{10-δ} (RP -LSCF)	0.255	388	~15	<i>Nano Energy</i> 2017, 40, 115
A-PBCCF-H NF	0.232	410	~14	<i>Nano Energy</i> 2017, 32, 247
NiO-(La _{0.613} Ca _{0.387}) ₂ NiO _{3.562} (NiO-LCN)	0.36	373	~11	<i>Nano Energy</i> 2015, 12, 115
SrSc _{0.025} Nb _{0.025} Co _{0.95} O _{3-δ} (SSNC)	0.36	~380	~10	<i>Mater. Horiz.</i> 2015, 2, 495
BaCo _{0.7} Fe _{0.2} Sn _{0.1} O _{3-δ} (BCFS)	0.232	~420	~4.8	<i>Adv. Sci.</i> 2016, 3, 1500187

Table S3. O 1s XPS peak deconvolution results.

Electrocatalysts	lattice O ²⁻	-OH or O ₂	H ₂ O or CO ₃ ²⁻
SCF800	19.1%	76.5%	4.4%
SCF1000	9.8%	86.7%	3.5%
SCF1200	5.6%	89.9%	4.5%

O 1s XPS spectra can be deconvoluted into three different characteristic peaks, i.e., lattice oxygen species (~529.6 eV), hydroxyl groups or the surface adsorbed oxygen (~531.2 eV) and adsorbed molecular water or carbonates (~532.4 eV).

References

- [S1]. Y. Zhu, H. Tahini, Y. Wang, Q. Lin, C. Doherty, Y. Liang, Y. Liu, X. Li, J. Lu, S. C. Smith, C. Selomulya, X. Zhang, Z. Shao and H. Wang, *J. Mater. Chem. A.* 2019, 7, 14222.
- [S2]. Y. Zhu, W. Zhou, Y. Zhong, Y. Bu, X. Chen, Q. Zhong, M. Liu and Z. Shao, *Adv. Energy Mater.* 2017, 7, 1602122.
- [S3]. N. Reiko, J. Stöhr and Y. U. Idzerda, *Phys. Rev. B* 1999, 59, 6421.
- [S4]. D. Guan, J. Zhou, Z. Hu, W. Zhou, X. Xu, Y. Zhong, B. Liu, Y. Chen, M. Xu, H. J. Lin, C. T. Chen, J. Wang and Z. Shao, *Adv. Funct. Mater.* 2019, 29, 1900704.
- [S5]. W. T. Hong, K. A. Stoerzinger, Y. L. Lee, L. Giordano, A. Grimaud, A. M.

Johnson, J. Hwang, E. J. Crumlin, W. Yang and Y. Shao-Horn, *Energy Environ. Sci.* 2017, **10**, 2190.